Local magnetic properties of γ-Fe-Mn alloys

C. Paduani
Departamento de Física, Universidade Federal de Santa Catarina, UFSC, Florianópolis CEP 88040-900, SC, Brazil

J. C. Krause
Instituto de Física, Universidade Federal do Rio Grande do Sul, UFRGS, Porto Alegre CEP 91501-970, RGS, Brazil
(Received 23 October 1997; revised manuscript received 9 January 1998)

The electronic structure of disordered Fe-Mn alloys in the fcc phase are investigated in spin-polarized cluster calculations with the first-principles discrete variational method. The effect on the local properties of the addition of Mn atoms in the fcc iron host is investigated. The introduction of one Mn atom in the immediate neighborhood of the iron site in this matrix reduces both the local moment (μ) and the contact field (H_c). An isolated Mn atom in this host exhibits a moment of about $-1.1\mu_B$ and a H_c value of about -9 kG. The calculations indicate that at the equiatomic composition is expected an abrupt decrease for the magnetic moment at iron sites, which is known from experimental results. [S0163-1829(98)03825-9]

I. INTRODUCTION

In the last decades several theoretical schemes have been employed to study the magnetic behavior of metallic systems. In this matter the iron alloys and compounds especially have been the focus of attention of the research. An overwhelming quantity of experimental work has been done in disordered iron alloys. Among them, the antiferromagnetic Fe-Mn alloys with the fcc structure were intensively investigated, mainly to explore the antiferromagnetism of the fcc iron.[1,2] The formation of magnetic moments and the nature of the interactions in fcc iron has been the subject of discussion for a long time. Since the early efforts to investigate the stability of this iron phase, the γ-FeMn alloys have been used in experimental works as being more adequate to describe the fcc iron properties.

The experimental results have indicated an antiferromagnetic ordering for these alloys at low temperatures.[3–14] However, the magnetic properties of these alloys showed a complex and unusual behavior. At the same time the extrapolation of the obtained quantities to the pure iron side shed some light on the magnetic structure of γ-Fe, the understanding of the observed properties of the γ-FeMn alloys revealed to be not so easy. In fact, there still remains nowadays some lack in the full description of its properties.

In Fe-Mn alloys, the fcc γ phase has been found to occur in the range 25–55 at. % of Mn.[7] The alloys are antiferromagnetic at room temperature. From 20 at. % Mn up to about 25 at. % Mn the γ phase coexists with the ϵ phase (hcp). Below 20 at. % Mn the γ phase is paramagnetic and coexists with the ferromagnetic α phase (bcc) at RT. A small amount of carbon ($\lesssim 1$ at. %) and an appropriate heat treatment were revealed to be sufficient to retain the fcc structure in iron alloys.[14] The experimental results have indicated that the magnetic moments on Fe and Mn atoms behave in fairly different ways with the temperature.[9,11] Besides, above 30 at. % Mn, Mössbauer effect measurements have shown that the hyperfine magnetic field at iron sites is well defined and is composition independent, even in low temperatures.[9–11,14]

A remarkable result is that the average magnetic moment per atom decreases, but the Néel temperature increases by increasing the manganese concentration. However, since the Fe-Mn interaction seems to be weak, it is the Mn-Mn interaction which is expected to vary with composition.[9,11] Further, the electronic specific-heat coefficient increases steeply by increasing iron concentration. Concerning the strong dependence of the local moment with the composition, it is expected that the Fermi surface in these alloys may be situated at the position where the plot of the density of states versus energy has a steep slope. Moreover, the neutron diffuse scattering cross section results indicated indeed the existence of a short-range order between Fe and Mn atoms in these alloys.[10]

Starting from the manganese-rich end in the phase digram, the Néel temperature increases almost discontinuously when iron concentration exceeds about 40 at. %, which suggests that a significant change in the magnetic structure occurs.[12] Mössbauer measurements indicate that the internal field appears only when the concentration exceeds 20 at. % Mn, and above 30 at. % Mn it becomes composition independent ($H_c \approx 33$ kG), which was argued as if the atomic moment of Fe atoms are saturated, once it appears.[12]

The average magnetic moment has a complicated dependence on composition and shows a minimum at 50 at. % Mn. The experimental results indicate also that the antiferromagnetic ordering in the intermediate region of composition comes from the formation of a magnetic energy gap and suggests that the shape of the Fermi surface plays an essential role.[12] According to these authors, the Néel temperature dependence on the concentration indicates a localized moment for Fe atoms which is weakly coupled with the magnetic moment of Mn atoms. Moreover, the magnetic structure of these alloys should be determined by the manganese band. The experimental results indicate also that the observed increase of the magnetic moment in the intermediate region of composition is due to the increase of the magnetic moment of Mn atoms, which comes from the decrease of the band width of the manganese with the reduction of manganese content. The magnetic state of Mn atoms at the iron-rich

alloys is not well known yet, and one suggests that it should be in a nonmagnetic state.

The band structures of γ-Mn and γ-Fe were studied by Asano and Yamashita, by means of Green-function techniques with the Slater exchange approximation.[13] With a random-phase approximation treatment, and extending the Mueller's combined interpolation scheme, the antiferromagnetism in the fcc phase was examined within the limit of the rigid-band approximation. In this picture, the magnetic moments of both fcc Mn and fcc Fe were obtained as 2.3 and $0.7\mu_B$, respectively, besides an antiferromagnetic ordering for these phases occurs at low temperatures. Their calculations indicate also that the local situation seems to be very important and the band theory is not applicable in this case as well, because a uniform exchange approximation does not hold there in a strict sense. They ascribed a gap-type antiferromagnetism in γ-FeMn alloys, where the Néel temperature is expected to have a deep connection with the magnitude of the magnetic energy gap or magnetic moment, considering that the appearance of this gap is caused by the existence of a long-range order in spin fluctuation.

More recently, cluster calculations in fcc iron indicates a magnetic moment of about $0.70\mu_B$, an isomer shift of about 0.14 mm/s, and a H_c value of about 60 kG at the iron site in this phase.[15] The results of the calculations showed a strong dependence of both μ and H_c values with lattice spacing.

In this work the local magnetic properties and the electronic structure of fcc iron clusters with the introduction of Mn atoms are investigated with the discrete variational (DV) method,[16] in the formalism of the local-spin-density approximation of the density-functional theory, where the exchange-correlation term of von Barth–Hedin is adopted.[17] The DV method is well described elsewhere in the literature cited above. In the following sections we concentrate on a discussion of the results.

II. CALCULATIONAL DETAILS

The scheme of the DV method consists of solving the self-consistent one-particle Kohn-Sham equations, where the molecular orbitals are expanded on a basis of atomic numerical orbitals, which are generated by solving the self-consistent atom problem, with the spherically averaged potential around each atom. The functional dependence of the Coulomb potential usually has a large computational cost, but is largely bypassed by the DV method which replaces the exact molecular charge density by a self-consistent multicenter-multipolar representation.[18]

The molecular clusters were built up with 19 atoms, including two shells of neighbors, adopting the known experimental value of 6.7805 a.u. for the lattice spacing of fcc iron.[19] The origin of coordinates is at the face-centered site. The minimal basis is adopted, which includes $1s$-$4p$ orbitals for both Fe and Mn atoms. The potential atoms in the crystal region are truncated at about -0.2 eV above the Fermi energy in order to prevent electron migration from the cluster toward low-lying energy states in the crystal. The microcrystal is embedded in the potential crystal consisting of about 350 atoms. This embedding scheme is well-described elsewhere in the literature.[20] All the electrons in the cluster have variational freedom during the self-consistent cycles.

The probe atom, which is expected to exhibit bulklike properties, is the central atom of each cluster. The eletron-s spin density at the iron nuclei is obtained in a special integration scheme on a variational point grid of about 250 points per atom.[20] The contribution to the contact field for the deep $1s$, $2s$, and $3s$ core orbitals are obtained by means of an atomic calculation in the X_α approximation, by using the converged electronic configurations from the molecular calculations, after an appropriate diagonal weighed population analysis in order to obtain the atomic-orbital populations. This treatment is advisable considering the finite-cluster size, and there is no sufficient delocalization of the wave functions taking place. The conduction-electron contribution is obtained directly from the molecular orbitals. The electron-s charge density at the iron nuclei, necessary to evaluate the isomer shift (IS), is obtained directly from the molecular calculation, being that the only relevant contribution comes from $3s$ and $4s$ orbitals.[21] The results are obtained relative to α-Fe.

III. DISCUSSION

Figures 1(a)–1(c) display the partial density of states (PDOS) for the central iron atom which is located at a face-centered site. In Fig. 1(a) one can see how the $3d$ states are accumulated near the Fermi surface, with a very pronounced peak for spin-down states just below E_F. Virtual bond states are mostly available for spin-up d electrons with energy values close to E_F. The $4s$ and $4p$ states are shifted to lower energies, and are almost depolarized and somewhat localized in energy [Figs. 1(b) and 1(c)]. The topological features of these diagrams indicate that fcc iron satisfies the Stoner criterion. Owing to the fact that it exhibits a high DOS at the Fermi level makes it energetically favorable to the ordering into a magnetic state through the exchange interaction which could split apart the majority- and minority-spin subbands.

Figures 2(a)–2(c) display the PDOS for the Mn atom as an isolated impurity in the fcc iron host. The $3d$ spin-up states are more localized in the energy space, with a resonance at the Fermi energy. The latter establishes a common band with the iron states, with a similar structure [Figs. 2(b) and 2(c)]. The $3d$ PDOS for the central iron atom with eight Mn atoms nearest-neighbors (NN) is showed in Fig. 3(a), where one can see the tiny polarization for these states. In fact, the small magnetic moment obtained in this case is almost entirely due to the conduction band, which contributes about two-thirds of the overall local moment, being that the $4p$ electrons contribute about 50% more than the $4s$ electrons. Replacing the Mn atoms for the iron atoms in the first shell of neighbors increases the polarization of the conduction band. From this result, one should expect also an increase of the transition temperature in this case. In fact, the experimental results show an increase of the ordering temperature by increasing the manganese concentration in these alloys, which reaches a maximum at the equiatomic composition.[14,12]

In Table I is shown the calculated results for the local moment μ, the contribution from conduction electrons μ_c $(4s+4p)$, the charge transfer Q, the magnetic hyperfine field (Fermi contact term) H_c, and the isomer shift (IS), for the central atom of each cluster. For fcc iron $\mu=0.69\mu_B$,

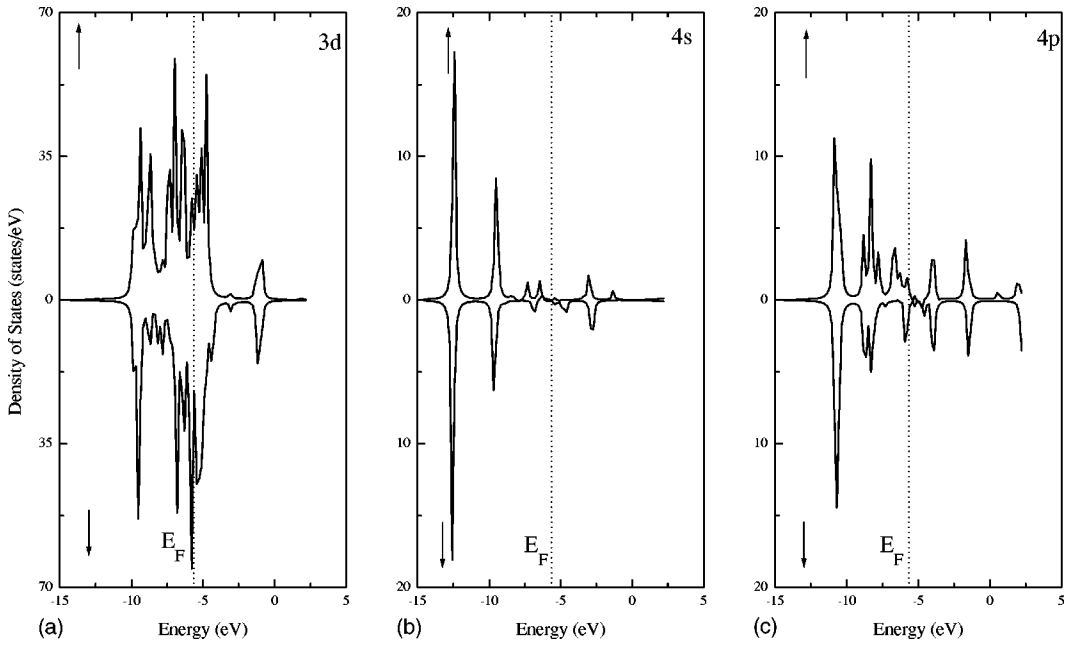

FIG. 1. $3d$ PDOS for pure fcc iron (a), $4s$ (b), and $4p$ (c).

and for an isolated Mn atom in this matrix, $\mu = -1.1\mu_B$ (antiferromagnetically coupled to the surrounding iron atoms in that plane). The μ_c value for the Mn is -0.21, parallel to the $3d$ contribution to the total magnetic moment. This magnitude is larger than that from the iron sites (0.19), and has reversed orientation.

The introduction of one Mn atom in the immediate neighborhood of an iron site causes a reduction in the local moment, mostly due to the reduction of the contribution from $3d$ electrons. However, by increasing the number of Mn NN atoms one observes an increase of the magnetic moment up to four Mn NN atoms, which has the largest μ value. With eight Mn NN atoms, which corresponds to the equiatomic composition in the alloys, we observe an abrupt decrease in the μ value. This feature is confirmed by experimental results.[12] Actually, it is interesting to observe that, in this case, the conduction-band contribution is rather strong, giving indeed the major contribution for the local moment. This suggests an enhancement of the coupling between the Fe and Mn atoms, which in turn should increase the critical temperature. In fact, at the equiatomic composition, we observe a maximum in the transition temperature and a minimum for the magnetic moment.[12]

Furthermore, with the first shell of neighbors completely filled up with Mn atoms, the μ value is higher than for pure fcc iron, which is also confirmed by experimental results at higher manganese concentrations in these alloys. An enhancement of the conduction-electron contribution to the lo-

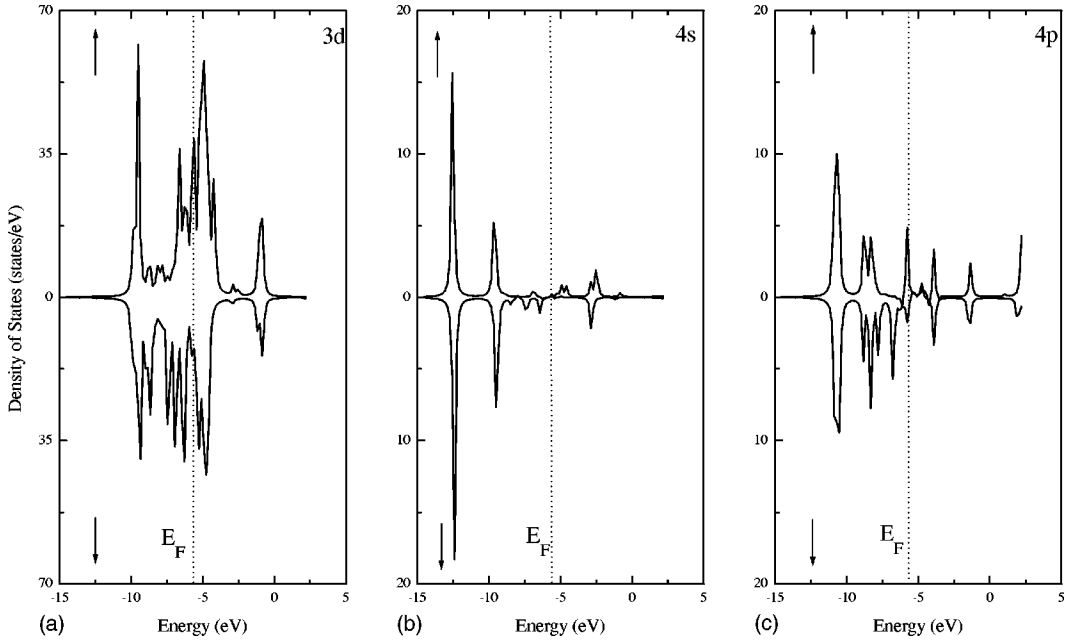

FIG. 2. $3d$ PDOS for the central Mn atom (a), $4s$ (b), and $4p$ (c).

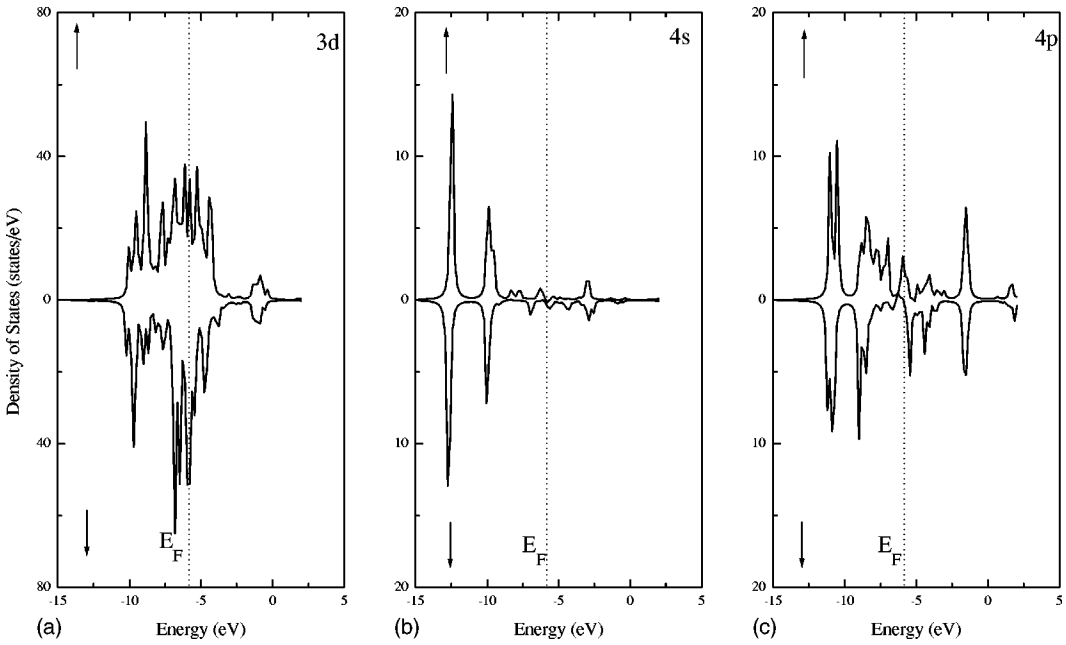

FIG. 3. $3d$ PDOS for eight Mn NN atoms (a), $4s$ (b), and $4p$ (c).

cal moment is also observed in this case. Our results indicate that the iron magnetic moment is quite sensitive to the occupancy of the neighboring sites, and the local symmetry has a strong effect on the magnetic polarization at the iron sites in this matrix. With six Mn NNN atoms (second shell of neighbors) in Table I, one observes about the same IS and μ values at the central iron atom as for the case of one Mn NN atom, whereas the contact field is little affected compared to the pure fcc iron, which indicates a short-range effect for the latter.

As far as the charge transfer is concerned, the ionization of the iron sites is quite sensitive to the atomic environment in this phase and is always positive, which indicates that the Fe atoms act as donors for the electrons. On the other hand, the isolated Mn atom suffers an expressive outflow of electrons, showing also the character of donor for electrons in these sites. We observe in Table I that a minimum occurs for Q at the same time as μ reaches a maximum.

TABLE I. Calculated results for the central atom of each cluster: total magnetic moment (μ), the contribution from the conduction band $4s+4p$ (μ_c), the ionization (Q), the hyperfine magnetic field (H_c), and the isomer shift (IS).

Cluster	$\mu(\mu_B)$	μ_C	Q	H_c (kG)	IS (mm/s)
$FeFe_{12}Fe_6$	0.69	0.19	0.26	60	0.14
$MnFe_{12}Fe_6$	−1.10	−0.21	0.38	−9	
$FeFe_{11}MnFe_6$	0.27	0.17	0.17	10	0.10
$FeFe_{10}Mn_2Fe_6$	0.62	0.22	0.19	55	0.08
$FeFe_8Mn_4Fe_6$ [a]	2.15	0.41	0.09	19	0.06
$FeFe_8Mn_4Fe_6$ [b]	2.71	0.67	0.01	69	0.03
$FeFe_4Mn_8Fe_6$	0.34	0.26	0.07	97	0.05
$FeMn_{12}Fe_6$	1.00	0.25	0.10	90	0.06
$FeFe_{12}Mn_6$	0.28	0.18	0.26	55	0.12

[a] D_{2h}.
[b] D_{4h}.

The H_c field at the iron sites is strongly influenced by the atomic environment and exhibits rather complex behavior. The experimental results reported in the literature indicate a constant value for H_c within the range of concentration above 25 at. % Mn. In fact, this accounts for the average magnetic hyperfine field. Actually, it was also reported that at 80 K this field increases from 25 kG for 12 at. % Mn almost linearly up to about 38 kG at 30 at. % Mn. There, the average H_c value is composition independent thereafter, but the contribution of each configuration around the iron sites was identified as changing with the concentration.[14] At 80 K, in the distribution obtained for the average magnetic field, above 25 at. % Mn, the peaks representing the field values, corresponding to particular arrangements of the atomic environment around the iron sites, were identified at about 15, 32, 39, 47, 50, and 58 kG. In spite of the somewhat high μ value for the configuration with four Mn NN atoms, we observed a small H_c value. This arises from the fact that, in this case, the contribution to the density of spin of electrons s at the iron nuclei has opposite signals for conduction and core orbitals, and that the core electrons contribution is reduced.

In the present calculations we verified a strong dependence of H_c with the local symmetry as well as with the composition, and a positive sign in all cases. Furthermore, we estimate a reduction of about 50 kG in the H_c value at the iron sites with the addition of one Mn atom in its immediate neighborhood. The isolated Mn atom in the fcc iron host exhibits a small H_c value of about -9 kG, against a value of about 60 kG for the pure fcc iron. The largest H_c value occurs when a minimum is observed for the local moment. Moreover, according to the present calculations, no linear correlation is expected between H_c and the long-range order magnetization parameter.

In Table I we observe that the IS values decrease almost continuously with the addition of Mn atoms in the first shell of neighbors around the iron sites. For pure fcc iron it is about 0.14 mm/s, relative to α-iron (bcc). The calculated IS

value for eight Mn NN atoms is close to the experimental value obtained at 4.2 K in a single crystal at the equiatomic composition.[8] The lowest IS value occurs together with the minimum for Q, which belongs to a particular environment around the iron site with four Mn NN atoms, at the same time where μ is at a maximum in Table I. In all those cases IS has positive values and is very sensitive to the local symmetry in this matrix.

IV. CONCLUSIONS

First-principles calculations are performed with the molecular cluster DV method to investigate the electronic structure and local magnetic properties of Fe-Mn alloys in the fcc disordered phase. The obtained PDOS diagrams showed that the Fermi surface in these alloys is located at the position where there is a steep slope in the density of states, which indicates a strong dependence of the magnetic moment with the composition, for both the Fe and Mn atoms, which is confirmed by experimental results. The introduction of one Mn atom in the immediate neighborhood of an iron site causes an abrupt decrease in both the hyperfine magnetic field (contact Fermi term) and the local magnetic moment. The contribution from the conduction electrons for the total magnetic moment follows the behavior of that from localized electrons, which are ferromagnetically coupled to them. Our calculations indicate that around the equiatomic composition in these alloys is expected an increase of the ordering temperature, which is confirmed by experimental results. The contact field is quite sensitive to the local symmetry in this phase. Finally, our results confirm that the magnetic moments of both the Fe and Mn atoms depend on the concentration in this phase, and the Mn atom is in a magnetic state at the iron-rich end.

ACKNOWLEDGMENTS

We thank the NPD of UFSC for the computational support. This work was supported by CNPq and FINEP, Brazilian agencies.

[1] H. Umebayashi and Y. Ishikawa, J. Phys. Soc. Jpn. **21**, 1281 (1966).
[2] F. J. Pinski, J. Staunton, B. L. Gyorffy, D. D. Johnson, and G. M. Stocks, Phys. Rev. Lett. **56**, 2096 (1986).
[3] S. C. Abrahams, L. Guttman, and J. S. Kasper, Phys. Rev. **127**, 2052 (1962).
[4] M. F. Collins and G. G. Low, Proc. Phys. Soc. London **86**, 535 (1965).
[5] I. A. Campbell, Proc. Phys. Soc. London **89**, 71 (1966).
[6] U. Gonser and H. G. Wagner, Hyperfine Interact. **24**, 769 (1985).
[7] M. Hansen and K. Ardenko, *Constitution of Binary Alloys* (McGraw-Hill, New York, 1958).
[8] S. J. Kennedy and T. J. Hicks, J. Phys. F **17**, 1599 (1987).
[9] Y. Ishikawa and Y. Endoh, J. Phys. Soc. Jpn. **23**, 205 (1967).
[10] Y. Ishikawa and A. C. Gossard, J. Appl. Phys. **39**, 1318 (1968).
[11] T. Hashimoto and Y. Ishikawa, J. Phys. Soc. Jpn. **23**, 213 (1967).
[12] Y. Endoh and Y. Ishikawa, J. Phys. Soc. Jpn. **30**, 1614 (1971).
[13] S. Asano and J. Yamashita, J. Phys. Soc. Jpn. **31**, 1000 (1971).
[14] C. Paduani, E. G. da Silva, and G. A. Perez-Alcazar, Hyperfine Interact. **73**, 233 (1992).
[15] C. Paduani and E. G. da Silva, J. Magn. Magn. Mater. **134**, 161 (1994).
[16] D. E. Ellis, Int. J. Quantum Chem. **2S**, 35 (1968); D. E. Ellis and G. S. Painter, Phys. Rev. B **2**, 2887 (1970); G. S. Painter and D. E. Ellis, Phys. Rev. B **1**, 4747 (1970); E. J. Baerends, D. E. Ellis, and P. Ros, Chem. Phys. **2**, 41 (1973).
[17] U. von Barth and L. Hedin, J. Phys. C **5**, 1629 (1972).
[18] B. Delley and D. E. Ellis, J. Chem. Phys. **76**, 1949 (1982).
[19] J. B. Newkirk, Trans. Am. Inst. Min. Metall. Pet. Eng. **209**, 1214 (1957).
[20] C. Umrigar and D. E. Ellis, Phys. Rev. B **21**, 852 (1980); D. E. Ellis, G. A. Benesh, and E. Byron, *ibid.* **20**, 1198 (1979); B. Delley, D. E. Ellis, and A. J. Freeman, J. Magn. Magn. Mater. **30**, 71 (1982).
[21] J. V. Mallow, A. J. Freeman, and J. P. Desclaux, Phys. Rev. B **13**, 1884 (1976).